Structural and functional brain changes in acute Takotsubo Syndrome

Hilal Khan, MB BCh, BAO, MRCP[1]

David T. Gamble, MB ChB MRCP[1]

Amelia Rudd, RDCS, BSE[1]

Alice M. Mezincescu, MD, PhD, MRCP[1]

Hassan Abbas, MBChB, BSc, MRCP[1]

Awsan Noman, MBChB, MRCP, MD, FESC[1]

Andrew Stewart, MBChB, FRCP, PhD[1]

Graham Horgan, BSc, PhD[1]

Rajeev Krishnadas, MBBS, DNB, MD, PhD, FRCPsych[2]

Christopher Williams, MBChB, BSc, MMedSc, MD, Hon Fellow BABCP, FRCPsych,[2,3]

Gordon Waiter, CPhys, FInstP, CSci, MIPEM, PhD[1]

Dana K Dawson MD, FRCP, D. Phil, FESC[1]

[1] University of Aberdeen**,** Aberdeen, United Kingdom

[2]University of Glasgow, Glasgow, United Kingdom

[3]Five Areas ltd, Glasgow, United Kingdom

Sources of Funding: This work was supported by NHS Grampian Endowment EA9667/ES868

Disclosures: None.

Address for Correspondence: Hilal M. W. Khan, MB BCh, BAO, MRCP, Aberdeen Cardiovascular and Diabetes Centre, Room 1:03 Ashgrove House, Foresterhill, University of Aberdeen, UK

Tel: +44 1224 559573, Fax: +44 1224 437971

Email: hilal.khan@abdn.ac.uk

Total Word Count: 4982

Keywords: cardiomyopathy, takotsubo, brain, imaging

Abstract

Background: Takotsubo syndrome mimics an acute myocardial infarction, typically in the aftermath of mental or physical stress.

Objectives: The mechanism by which emotional processing in the context of stress leads to significant cardiac injury is poorly understood, therefore a full exploration of brain structure and function in takotsubo syndrome patients merits investigation.

Methods: Twenty-five acute (< 5 days) takotsubo patients and 25 controls were recruited into this observational cross-sectional study. Surface-based morphometry was carried out on brain magnetic resonance imaging (MRI) scans to extract cortical morphology based on volume, thickness and surface area using Freesurfer. Cortical morphology general linear models were corrected for age, gender, photoperiod and total brain volume. Resting state functional MRI and diffusion tensor tractography images were pre-processed/analysed with FMRIB's Diffusion Toolbox/ CONN toolbox.

Results: There was significantly smaller total white matter and subcortical grey matter volumes in takotsubo ($p<0.001$), with smaller total brain surface area but increased total cortical thickness (both $p<0.001$). Individual grey matter regions (hippocampus and others) were significantly smaller in takotsubo (<0.001); only thalamus and insula were larger ($p<0.001$). There was significant hyper- and hypo-functional connectivity in multiple areas including thalamus-amygdala-insula and basal ganglia ($p<0.05$). All structural tractography connections were increased in takotsubo ($p<0.05$).

Conclusions: We showed smaller grey and white matter volumes driven by smaller cortical surface area, but increased cortical thickness and structural tractography connections with bi-directional changes in functional connectivity linked to emotion, language, reasoning,

perception and autonomic control. These are interventional targets in takotsubo patients' rehabilitation.

Abbreviations

LGA: Lesion Growth Algorithm

LST: Lesion Segmentation Tool

MNI: Montreal Neurological Institute

CONN: Functional Connectivity Toolbox

ART: ARtifact Detection Tools

FDT: Functional Magnetic Resonance Imaging of the Brain Diffusion Toolbox (FDT)

BET: Brain Extraction Toolbox

DTIFIT: Diffusion Tensor Imaging Fit Toolbox

BEDPOSTX: Bayesian Estimation Of Diffusion Parameters Obtained Using Sampling Techniques

PROBTRACKX: Probabilistic Tracking with Crossing Fibres

Introduction

Takotsubo syndrome is an acute heart failure cardiomyopathy mimicking an acute myocardial infarction in its presentation (1). Typically, it occurs in the aftermath of intense psychological or physical stress, affecting women in over 90% of cases. The mechanism by which emotional processing in the context of stress leads to significant cardiac injury and acute left ventricular dysfunction has yet to be elucidated. Therefore, a full exploration of the brain structure and function in takotsubo syndrome merits investigation.

A recent retrospective analysis using $^{18}F^{-}$Fluorodeoxyglucose PET-CT examination of a patient cohort investigated for cancer showed higher amygdala activity (an area involved in the experiencing of emotions) in subjects who subsequently developed takotsubo syndrome after 2 years (2), suggesting the possibility of a premorbid state affecting the brains of patients with takotsubo syndrome. Several reports have shown structural and functional differences of the brain limbic system and areas involved in regulating the autonomic nervous system in patients with takotsubo syndrome, suggesting impaired interaction between centres responsible for processing emotional inputs and the autonomic nervous system (3-5). All these studies, except one(5), included patients at variable, later stages after the acute presentation, possibly masking phasic variations that occur thereafter, which may be important markers of recovery or sustained predisposing risk. Furthermore, one large international registry reported a significant stroke outcome in takotsubo patients(6), and recently white matter hyperintensities (which reflect small vessel disease) have been linked to an increased risk of developing future stroke (7).

In this study we explore a whole-brain magnetic resonance imaging (MRI) investigation of acute changes in takotsubo presenters. Specifically, we examined the cortical surface areas, cortical thickness, white matter hyperintensity volumes as well as grey matter volumes, the

structural connectivity network of grey matter centres (tractography) using diffusion tensor imaging and their resting state connectivity using functional magnetic resonance imaging (fMRI), compared to a matched control population.

Methods

Study populations

Between October 2020-July 2021, we recruited 25 patients with acute takotsubo syndrome who underwent brain magnetic resonance imaging (MRI) and validated psychology questionnaire assessment during the first 5 days post-diagnosis (23 of these patients were recruited consecutively from a single centre and 2 were referred from external collaborating centers). Exclusion criteria included patients too frail to participate, those with significant neurological diseases or dementia or contraindications/intolerance to magnetic resonance imaging (MRI). Patients were identified by the attending cardiologist based on history, electrocardiogram, biomarker, echocardiography, coronary angiography and cardiac MRI findings. All patients were screened by cardiac MRI to ensure the patient had not had a myocardial infarction or other cardiomyopathy. In addition, all patients had follow-up cardiac imaging to ensure resolution of wall motion abnormalities. All patients met the European Society of Cardiology criteria for diagnosis of takotsubo syndrome. We selected a group of age, gender, medical and mental health comorbidity matched controls from participants who had identical neurological investigations as part of the STratifying Resilience and Depression Longitudinally (STRADL) study(8). This study recruited participants with and without depression who completed the same psychology questionnaires and had MRI brain scans performed using the exact same sequences as in the takotsubo syndrome patients. The same magnetic resonance scanner equipment was used to acquire the imaging data and the same software version was utilised for data analysis of both patient cohorts. All patients gave written informed consent. The study was approved by the local research ethics committee(20/SC/0305).

Psychology Questionnaires

All patients were given the Hospital Anxiety and Depression Scale (HADS)(9) and the Eysenck Personality Questionnaire-Revised (EPQ-R)(10) to complete on the day of MRI scanning.

Environmental variable-photoperiod

To adjust for seasonal changes in brain volumes, all brain volumes were corrected for photoperiod(11). The photoperiod of the scanning centre was determined by using the United States Naval observatory online data repository and calculated by subtracting the time of sunset from the time of sunrise on the day of scanning for each participant(12).

Brain Magnetic Resonance Imaging protocol

Brain MRI was performed on a 3T Philips Achieva TX-series MRI system (Philips Healthcare, Best, Netherlands) based in the biomedical imaging centre at Aberdeen Royal Infirmary with a 32-channel phased-array head coil. **T1** weighted fast gradient echo images (160 sagittal slices, repetition time (TR) = 8.2 ms, echo time (TE) = 3.8 ms, TI = 1031 ms, fractional anisotropy (FA) = 8°, field of view (FOV) = 240 mm, matrix size = 240 × 240, voxel size = 1.0 × 1.0 × 1.0 mm^3), **diffusion tensor images (DTI)** (60 axial slices, TR = 7010, TE = 90 ms, FA = 90°, FOV = 220 mm, matrix size = 96 x 94, Voxel size = 2.3 x 2.3 x 2.3 mm^3, 64 non-collinear gradient directions (b = 1200 s/mm2), eight unweighted (b = 0)), **resting-state functional MRI** (fMRI) (32 axial slices, TR = 1560 ms, TE = 26 ms, FA = 70°, FOV = 217 mm, matrix size = 64 × 64, voxel size = 3.4 × 3.4 × 4.5 mm^3), and **Fluid Attenuation Inversion Recovery (FLAIR)** (160 sagittal slices, TR = 8000 ms, TE = 349 ms, TI = 2400 ms, FA = 8°, FOV = 240 mm, matrix size = 240 × 238, voxel size = 1.0 × 1.0 × 1.0 mm^3) were acquired in a 25 min protocol.

White matter hyperintensities

Automated lesion segmentation was performed using the lesion growth algorithm (LGA) provided by lesion segmentation tool (LST). LGA requires T1 and FLAIR images and outputs lesion probability maps, total lesion volume and number. An initial binary lesion map obtained by imposing a predetermined initial threshold (0.5) on the independent maps is then grown along hyperintense voxels in the FLAIR image. Total lesion volume was calculated from the lesion probability maps with a threshold of 0.5.

Volumetric, Surface area and Cortical thickness analysis for total and individual brain centre areas

Cortical reconstruction and volumetric segmentation were performed with the Freesurfer image analysis suite v7.1.1, which is freely available online(13). This involves several post-processing steps to output volume measurements which are well validated in the literature. Once the cortical models were complete, several deformable procedures were performed for further data processing and analysis and creation of a variety of surface-based data including surface area measurements. Cortical thickness was calculated from both intensity and continuity information from the entire three-dimensional MR volume in segmentation and deformation to produce representations of cortical thickness. Procedures for the measurement of cortical thickness have been validated against histological analysis and manual measurements(14).

Functional Connectivity

Resting state functional MRI (fMRI) was analysed using the CONN toolbox which allowed takotsubo patients to be compared with matched controls for differences in functional connectivity with a bandpass filter of 0.008–0.09 Hz. Six motion-corrected parameters were included in the generalised linear model. An ROI-ROI based analysis was performed on all brain regions included in CONN. All results were corrected for age and sex. The Pearson

correlation between clusters was calculated across all regions, The r value acquired for the Pearson correlation between every two regions was z-transformed and group differences were calculated on the z-transformed values with a two-sample t test. False discovery rate correction was used to correct for multiple comparisons at the cluster level and corrected $p < 0.05$ was considered significant.

Structural connectivity (tractography)

Diffusion tensor images (DTI) were pre-processed using the FMRIB's Diffusion Toolbox (FDT). We corrected for motion and geometrical distortion due to eddy currents using the eddy correct tool in FDT, taking the average of the eight b0 volumes as the reference image. Non-brain tissue from the average b0 image was removed using the FMRIB Brain Extraction Toolbox, BET. False discovery rate correction was used to correct for multiple comparisons using CONN toolbox at the cluster level and corrected $p < 0.05$ was considered significant.

Statistical analysis of Volumetric, Surface area and Cortical thickness

SPSS v27 was used to analyse the differences in volumetric data using the general linear model and multivariate analyses of the brain volumes were corrected for total brain volume, age, gender and photoperiod. Surface area was corrected for age, gender and total brain volume. Cortical thickness was corrected for age, gender and whole brain cortical thickness. Multiple correction testing was performed for brain volume, surface area and cortical thickness using the Bonferroni correction. A p value <0.05 after Bonferroni adjustment was considered statistically significant.

Results

Baseline demographics and the validated questionnaire scores of the fifty participants recruited in the study are shown in **Table 1**. The median age is 65 in the control group and 68 in the takotsubo syndrome group (p=0.809). There are 24 females and 1 male in each group (p=1.0) There is no significant difference in comorbidities including psychiatric illnesses apart from a small number of COPD patients in the takotsubo group (n=5, p=0.018). There were 40% of Takotsubo patients with an emotional trigger, 28% with a physical trigger and 32% with no obvious identifiable trigger. The median time to MRI scanning was 5 days in the takotsubo syndrome group. The mean left ventricular ejection fraction in the takotsubo syndrome group was 45±8.3 %. The HADS score was significantly higher in the patient group compared to controls (p<0.001). See **Table 1 in supplement** for detailed case description of patients.

White matter hyperintensities: there was no difference in either the number or total volume of white matter hyperintensity lesions between acute takotsubo syndrome patients and matched controls. (**Table 2 supplement**)

Surface area of individual brain regions: As seen from **Table 2 (and Table 3 in supplement)**, acute takotsubo patients have significantly smaller surface areas of several brain regions such as the left rostral anterior cingulate and the right and left insula. Overall, acute takotsubo patients had significantly smaller total, right and left hemisphere surface areas.

Cortical thickness of individual brain regions: **Table 2 (and Table 4 in supplement)** shows that patients with acute takotsubo have significantly larger cortical thickness in brain regions such as the right insula. In addition, they demonstrate significantly larger total right and left hemisphere cortical thickness.

Total and individual brain centre volumes: As seen from **Table 2 (and Table 5 in supplement)**, acute takotsubo patients had significantly smaller white matter and subcortical grey matter volumes, whilst their cortical grey matter was larger. In addition, there were numerous significant differences in many of the limbic centre brain volumes between acute takotsubo syndrome patients and matched controls, notably: left, right and total hippocampus, and the brainstem were all significantly smaller in acute takotsubo patients. Conversely, left, right and total thalamus and insula were larger in patients with takotsubo syndrome compared to matched controls ($p<0.001$).

Functional connectivity: As shown in **Figure 1**, there were multiple significantly increased (in red lines) and decreased (in blue lines) functional connectivity networks in takotsubo patients versus matched controls (all $p< 0.05$). Specifically, there was increased connectivity between either the right thalamus or the left thalamus and the left caudate and left nucleus accumbens, or between anterior cingulate cortex and the right cerebral cortex or between the left thalamus and the posterior cerebellum. Conversely, there was significantly decreased functional connectivity between the right thalamus and the right inferior frontal gyrus, or between the entire thalamus and the left amygdala, left insula, visual lateral and visual medial lobes, orbitofrontal cortex, inferior frontal gyrus, or between the left insula and the left caudate and thalamus.

Structural connectivity (tractography): As shown in **Figure 2**, there was a significant increase in all structural connectivity connections in takotsubo syndrome compared to matched controls, notably with absence of any reduced structural connections in takotsubo patients. Specifically, the right and left thalamus showed significantly increased structural connectivity to the temporal regions. The left insula had significantly increased structural connectivity to the right amygdala, right putamen, right posterior cingulate gyrus, right rostral anterior cingulate gyrus.

Discussion

This is the largest cohort of takotsubo syndrome patients whose acute brain phenotype has been investigated. All cases were examined during the acute phase (within 5 days of presentation) to allow benchmarking of any changes that may occur before or during the subsequent convalescent phase because of medications or other interventions. We find no evidence of cerebral small vessel disease, as evidenced by similar number and volume of white matter hyperintensities compared to controls. In this study takotsubo patients had greater cortical thickness but smaller cortical surface areas. In our cohort takotsubo patients had smaller total white matter, total subcortical grey matter volume and all individual grey matter brain centres except for the thalamus and insula which were larger, in either hemisphere or combined. Distinct bi-directional changes in functional connectivity were seen compared to matched controls in this study, and this occurs in the context of all structural tractography connections being significantly increased in takotsubo patients.

Anatomical Changes in Takotsubo Syndrome

It is well understood that there are different genes responsible for the development of cortical surface area as compared to cortical thickness(15). The radial hypothesis suggests that during early development the brain develops along columns with each column being associated with a certain function. The surface area is determined by the number of columns whereas cortical thickness is influenced by the number of cells within a column. Later in life, cortical thickness appears to be influenced by environmental factors such as alcohol consumption and smoking whereas cortical surface area appears to be regulated by unique developmental factors (16, 17). Therefore, both a genetic difference as well as an adaptive cortical re-organisation could be responsible for the findings seen in the brain of takotsubo patients compared to controls.

Smaller cortical surface area and greater cortical thickness was noticed in takotsubo patients in this study this is also seen in patients with major psychiatric disease such as major depression (18). In addition, smaller brain grey matter volumes especially hippocampal volumes which we observed in patients with takotsubo syndrome are also seen in patients with elevated levels of inflammation (19) and have been previously reported in the amygdala by Hiestand, albeit at a later time from the index presentation (20). The reduction in grey matter volumes were also shown by Dichtl et al (5), confirming the involvement of the grey matter in patients who develop takotsubo syndrome. Hiestand et al showed reduced cortical thickness in a cohort of takotsubo patients 1 year after the acute event - this is contrary to the results shown here and may be explained by the timeframe when scanning was performed in that study(20). Both depression and anxiety disorders are associated with elevated levels of inflammation (21). Systemic and myocardial inflammation is a well-recognised feature of takotsubo syndrome (22, 23), which raises the possibility that the changes we observed in the brain of takotsubo syndrome patients are potentially adaptive and related to inflammation.

White matter hyperintensity findings in this cohort would suggest that takotsubo patients have a similar risk of cognitive impairment, dementia and stroke as a matched control population (24). If the increased risk of stroke suggested by the international takotsubo registry (6) was assigned to the significant premorbid incidence of neurological disease of the patients included in this registry, it could mean that in the absence of pre-existent neurological disease the risk of subsequent stroke for takotsubo patients may not be as high as suggested by registries.

Functional and Structural Connectivity Changes in Takotsubo Syndrome

Brain activity and functional connectivity networks are intricately linked to their structural connectivity patterns, such as brain regions with high structural connectivity normally exhibit

high functional connectivity, whereas the converse is not necessarily true(25). In this study we show that both thalamic and insulae nuclei are greater in size and have increased structural connections. Some of these findings overlap with those seen in other conditions, such as: greater thalamic volumes seen in patients with major depression and suicidal ideation (26) or increased functional connectivity between thalamus-nucleus accumbens linked to emotional processing regulating the pain response(27) and also involved in attenuating cardiac injury during ischemic damage(28). We have previously noted that there are increased pro-inflammatory cytokines and inflammatory markers such C-reactive protein in patients with takotsubo syndrome (29). Once again, increased inflammation has been associated with reduced functional activation of the thalamus and insular cortex (30) such as those observed here.

It is therefore intriguing to see a reduction in functional connectivity in the context of enhanced structural connections, which implies that the reduction in functional connectivity is not due to abnormal structural connections. An inflammatory substrate hypothesis makes it easier to reconcile observations such as: reduced functional connectivity from the right thalamus to the right inferior frontal gyrus (language centre) or to the visual lateral cortex in takotsubo patients in this study - the first also observed in schizophrenia and linked to aberrant encoding of semantic memory (abnormal processing of auditory stimuli, fixity of thinking with low flexibility and high emotional distress) (31), whilst the latter also seen in patients with anorexia nervosa and linked to abnormal processing of visual stimuli, overvalued ideation(32).

A noteworthy finding in this study is the reduced functional connectivity between the left thalamus and the left insular cortex. Lesions in the left amygdala or left insular cortex are associated with a 5-fold increased risk of sudden cardiac death in patients with schizophrenia (33). In patients with left insular lesions there is loss of parasympathetic control and

sympathetic overactivity with an increased risk of cardiac injury and arrythmia (34). Stroke patients with left insular lesions had poorer cardiac outcomes and were more likely to have cardiac wall motion abnormalities on echocardiography in the absence of obstructive coronary artery disease (35). Left insular lesions induced in mice resulted in cardiac injury and elevated serum levels of noradrenaline. The extent of the insular injury corresponded to the degree of cardiac injury (36). A previous study of patients with takotsubo syndrome 2 years after the acute event however noticed increased functional connectivity in the left insular cortex. A biphasic response with initial reduced insular functional connectivity leading to loss of parasympathetic control followed by increased insular connectivity thereafter is a plausible explanation of maladaptive autonomic response in these patients (37). Dichtl et al showed similar findings with reduced functional connectivity of the insula during the acute period in keeping with the results seen in this study(5). Templin et al showed similar findings with reduced functional connectivity in the insular region(3). This recurring finding of abnormal insular function strongly suggests a role for this region in the pathogenesis of takotsubo syndrome.

Another interesting finding in takotsubo patients in this study is the reduced functional connectivity in the caudate, putamen and the pallidum with increased functional connectivity in the nucleus accumbens - these together form key parts of the basal ganglia. Abnormalities in the basal ganglia have been associated with altered vagal nerve function and an increased risk of both brady-arrythmias and atrial fibrillation (38, 39). Altered functioning in this area may contribute to arrhythmic presentations seen in acute takotsubo syndrome or in the development of subsequent atrial fibrillation (40).

We also observe reduced functional connectivity in the amygdala of patients with acute takotsubo similar to patients with a tendency to catastrophise events(41). Previous observations showed reduction in functional connectivity in the amygdala years after the

acute event. Together these findings would imply that this area of emotional processing is abnormal both during the acute phase and long term(3).

These findings would support the nitrosative stress theory of takotsubo syndrome whereby maladaptive brain responses to stress involving the thalamus-amygdala-insular pathways lead to loss of autonomic control over the nervous system leading to sympathetic overactivity, nitrosative stress and cardiac injury which contributes to the acute and chronic heart failure phenotype seen in takotsubo syndrome(22, 29, 42, 43). The overlap of many of the anatomical and functional brain findings in takotsubo patients with those seen in psychiatric conditions is intriguing particularly because patients with depression or schizophrenia also have decreased survival due to excess cardiac mortality.

Limitations

As this is an observational study it is not possible to apportion causality of the observations which are merely hypothesis-generating. Follow-up of the natural history of changes in the brain of takotsubo syndrome patients could provide further insight.

Conclusion

In the largest structural and functional brain study of acute takotsubo syndrome patients compared to matched controls we demonstrate smaller cortical surface area and greater cortical thickness, no increase in white matter hyperintensities, smaller grey matter centres except for the thalamus and insula which were larger (in either hemisphere or combined), enhanced structural tractography connections with distinct bi-directional changes in functional connectivity linked to emotion, mood, language, visual and auditory perception as well as autonomic control.

COMPETENCY IN MEDICAL KNOWLEDGE:

- In the acute phase of illness takotsubo syndrome patients demonstrate overall increased cortical thickness but smaller cortical surface areas, smaller white and grey matter volumes and smaller individual brain centre volumes, except thalamus and insula.
- Patients with takotsubo syndrome have no significant difference in white matter hyperintensities compared to controls implying absence of small vessel disease.
- Takotsubo syndrome patients show areas of functional hypoconnectivity in key brain regions involving the thalamus-amygdala-insula axis and basal ganglia which are responsible for higher-level functions (emotion, reasoning, language, perception), as well as autonomic regulation of the brain-heart axis.
- Patients with takotsubo syndrome have increased structural tractography connections compared to controls suggesting the abnormalities in functional connectivity are not due to abnormalities in structural connections.

TRANSLATIONAL OUTLOOK:

- The abnormalities in the thalamus-amygdala-insula and basal ganglia support the concept of higher-level function centres involvement in takotsubo syndrome and interventions aimed at modulating these may be of benefit.

Acknowledgements

Professor Mark Petrie, Consultant Cardiologist, Glasgow, Dr David Corcoran, Consultant Cardiologist, Glasgow, Prof Stephen Leslie, Consultant Cardiologist, Inverness for identifying patients recruited in this study. We would like to acknowledge NHS Grampian Endowment EA9667/ES868, BHF Project Grant no. PG/18/35/33786, "Physical Exercise and mental wellbeing rehabilitation for Acute StrEss-induced takotsubo cardiomyopathy: The PLEASE trial and The Welcome Trust for supporting the work used in this study.

References

1. Prasad A, Lerman A, Rihal CS. Apical ballooning syndrome (tako-tsubo or stress cardiomyopathy): A mimic of acute myocardial infarction. Am Heart J. 2008;155:408-17.

2. Radfar A, Abohashem S, Osborne MT*, et al*. Stress-associated neurobiological activity associates with the risk for and timing of subsequent takotsubo syndrome. Eur Heart J. 2021.

3. Templin C, Hanggi J, Klein C*, et al*. Altered limbic and autonomic processing supports brain-heart axis in takotsubo syndrome. Eur Heart J. 2019;40:1183-7.

4. Pereira VH, Marques P, Magalhaes R*, et al*. Central autonomic nervous system response to autonomic challenges is altered in patients with a previous episode of takotsubo cardiomyopathy. Eur Heart J Acute Cardiovasc Care. 2016;5:152-63.

5. Dichtl W, Tuovinen N, Barbieri F*, et al*. Functional neuroimaging in the acute phase of takotsubo syndrome: Volumetric and functional changes of the right insular cortex. Clin Res Cardiol. 2020;109:1107-13.

6. Templin C, Ghadri JR, Diekmann J*, et al*. Clinical features and outcomes of takotsubo (stress) cardiomyopathy. N Engl J Med. 2015;373:929-38.

7. Epstein A, Schilter M, Vynckier J*, et al*. Chronic covert brain infarctions and white matter hyperintensities in patients with stroke, transient ischemic attack, and stroke mimic. J Am Heart Assoc. 2022:e024191.

8. Habota T, Sandu AL, Waiter GD*, et al*. Cohort profile for the STratifying resilience and depression longitudinally (STRADL) study: A depression-focused investigation of generation scotland, using detailed clinical, cognitive, and neuroimaging assessment[version 2; peer review: 2 approved]. Wellcome Open Research. 2021;4.

9. Zigmond AS, Snaith RP. The hospital anxiety and depression scale. Acta Psychiatr Scand. 1983;67:361-70.

10. Eysenck SBG, Eysenck HJ, Barrett P. A revised version of the psychoticism scale. Personality and Individual Differences. 1985;6:21-9. Available from: https://www.sciencedirect.com/science/article/pii/0191886985900261.

11. Majrashi NA, Ahearn TS, Waiter GD. Brainstem volume mediates seasonal variation in depressive symptoms: A cross sectional study in the UK biobank cohort. Scientific Reports. 2020;10:3592. Available from: https://doi.org/10.1038/s41598-020-60620-3.

12. Http://Aa.usno.navy.mil/data/docs/RS_OneYear.php.

13. Http://Surfer.nmr.mgh.harvard.edu/.

14. Rosas HD, Liu AK, Hersch S*, et al*. Regional and progressive thinning of the cortical ribbon in huntington's disease. Neurology. 2002;58:695-701.

15. Panizzon MS, Fennema-Notestine C, Eyler LT*, et al*. Distinct genetic influences on cortical surface area and cortical thickness. Cereb Cortex. 2009;19:2728-35.

16. Momenan R, Steckler LE, Saad ZS, van Rafelghem S, Kerich MJ, Hommer DW. Effects of alcohol dependence on cortical thickness as determined by magnetic resonance imaging. Psychiatry Res. 2012;204:101-11.

17. Karama S, Ducharme S, Corley J*, et al*. Cigarette smoking and thinning of the brain's cortex. Mol Psychiatry. 2015;20:778-85. Available from: https://doi.org/10.1038/mp.2014.187.

18. Nemati S, Abdallah CG. Increased cortical thickness in patients with major depressive disorder following antidepressant treatment. Chronic Stress (Thousand Oaks). 2020;4:10.1177/2470547019899962. Epub 2020 Jan 14.

19. Tsai SY, Gildengers AG, Hsu JL, Chung KH, Chen PH, Huang YJ. Inflammation associated with volume reduction in the gray matter and hippocampus of older patients with bipolar disorder. J Affect Disord. 2019;244:60-6.

20. Hiestand T, Hänggi J, Klein C*, et al*. Takotsubo syndrome associated with structural brain alterations of the limbic system. J Am Coll Cardiol. 2018;71:809-11. Available from: https://www.sciencedirect.com/science/article/pii/S0735109717419425.

21. Krishnadas R, Cavanagh J. Depression: An inflammatory illness? J Neurol Neurosurg Psychiatry. 2012;83:495-502.

22. Scally C, Abbas H, Ahearn T*, et al*. Myocardial and systemic inflammation in acute stress-induced (takotsubo) cardiomyopathy. Circulation. 2019;139:1581-92.

23. Khan H, Gamble D, Mezincescu A, Abbas H, Rudd A, Dawson D. A systematic review of biomarkers in takotsubo syndrome: A focus on better understanding the pathophysiology. Int J Cardiol Heart Vasc. 2021;34:100795.

24. Debette S, Markus HS. The clinical importance of white matter hyperintensities on brain magnetic resonance imaging: Systematic review and meta-analysis. BMJ. 2010;341:c3666. Available from: http://www.bmj.com/content/341/bmj.c3666.abstract.

25. Damoiseaux JS, Greicius MD. Greater than the sum of its parts: A review of studies combining structural connectivity and resting-state functional connectivity. Brain Struct Funct. 2009;213:525-33.

26. Young KA, Bonkale WL, Holcomb LA, Hicks PB, German DC. Major depression, 5HTTLPR genotype, suicide and antidepressant influences on thalamic volume. British Journal of Psychiatry. 2008;192:285-9.

27. Harris HN, Peng YB. Evidence and explanation for the involvement of the nucleus accumbens in pain processing. Neural regeneration research. 2020;15:597-605.

28. Cheng Y, Chang Y, Chen W*, et al*. Cardioprotection induced in a mouse model of neuropathic pain via anterior nucleus of paraventricular thalamus. Nature Communications. 2017;8:826.

29. Scally C, Rudd A, Mezincescu A*, et al*. Persistent long-term structural, functional, and metabolic changes after stress-induced (takotsubo) cardiomyopathy. Circulation. 2018;137:1039-48.

30. Han KM, Ham BJ. How inflammation affects the brain in depression: A review of functional and structural MRI studies. J Clin Neurol. 2021;17:503-15.

31. Jeong B, Wible CG, Hashimoto R, Kubicki M. Functional and anatomical connectivity abnormalities in left inferior frontal gyrus in schizophrenia. Hum Brain Mapp. 2009;30:4138-51.

32. Scaife JC, Godier LR, Filippini N, Harmer CJ, Park RJ. Reduced resting-state functional connectivity in current and recovered restrictive anorexia nervosa. Frontiers in Psychiatry. 2017;8:30.

33. Scorza FA, Schmitt A, Cysneiros RM, Arida RM, Cavalheiro EA, Gattaz WF. Thalamic nuclear abnormalities as a contributory factor in sudden cardiac deaths among patients with schizophrenia. Clinics (Sao Paulo, Brazil). 2010;65:539-46.

34. Oppenheimer SM, Kedem G, Martin WM. Left-insular cortex lesions perturb cardiac autonomic tone in humans. Clin Auton Res. 1996;6:131-40.

35. Laowattana S, Zeger SL, Lima JAC, Goodman SN, Wittstein IS, Oppenheimer SM. Left insular stroke is associated with adverse cardiac outcome. Neurology. 2006;66:477.

36. Min J, Eric, Farooq MU FAU - Greenberg, Greenberg E FAU - Aloka, Feras, *et al*. Cardiac dysfunction after left permanent cerebral focal ischemia: The brain and heart connection. Stroke JID - 0235266.

37. Silva AR, Magalhaes R, Arantes C, *et al*. Brain functional connectivity is altered in patients with takotsubo syndrome. Sci Rep. 2019;9:4187-3.

38. Pchejetski D, Kenbaz M, Alshaker H, Jesudason K. Bradycardia and syncope as sole manifestations of a cranial lesion: A case report. Journal of medical case reports. 2020;14:24. Available from: https://pubmed.ncbi.nlm.nih.gov/32000857 https://www.ncbi.nlm.nih.gov/pmc/articles/PMC6993381/.

39. Cheng W, Li D, Yang Q, Hou Y. Relationship between abnormal vagus nerve tension and basal ganglia cerebral infarction induced paroxysmal atrial fibrillation. Asian Pacific Journal of Tropical Medicine. 2017;10:921-4. Available from: https://www.sciencedirect.com/science/article/pii/S199576451731177X.

40. El-Battrawy I, Cammann VL, Kato K, *et al*. Impact of atrial fibrillation on outcome in takotsubo syndrome: Data from the international takotsubo registry. Journal of the American Heart Association. 2021;10:e014059. Available from: https://doi.org/10.1161/JAHA.119.014059.

41. Timmers I, López-Solà M, Heathcote LC, *et al*. Amygdala functional connectivity mediates the association between catastrophizing and threat-safety learning in youth with chronic pain. Pain. 9000.

42. Nguyen TH, Neil CJ, Sverdlov AL, *et al*. Enhanced NO signaling in patients with takotsubo cardiomyopathy: Short-term pain, long-term gain? Cardiovasc Drugs Ther. 2013;27:541-7.

43. Surikow SY, Nguyen TH, Stafford I*, et al*. Nitrosative stress as a modulator of inflammatory change in a model of takotsubo syndrome. JACC Basic Transl Sci. 2018;3:213-26.

Figure Legends

Figure 1. Altered functional connectivity in takotsubo syndrome.

Diagrams A-H show multiple areas of functional hypoconnectivity associated with regulation of the autonomic nervous systems and regions of hyperconnectivity involving the anterior cingulate gyrus and the salience networks (all $p<0.05$). Colour bars represent the set t-value of the connections between which the two groups differ in connectivity strength (with extremes of red=hyper-connectivity and blue=hypo-connectivity).

Figure 2. Structural Connectivity of regions of interest based on DTI differences between acute takotsubo syndrome and matched controls.

Colour bars represent the set t-value of the connections between which the two groups differ in connectivity strength, only enhanced structural connections were seen in takotsubo patients (all $p<0.05$).

Central Illustration: Brain-heart axis in takotsubo syndrome

Figure A shows increased cortical thickness and reduced surface area in takotsubo Syndrome. **Figure B** demonstrates larger volume thalamus and insula in takotsubo syndrome compared to controls. **Figure C** shows structural and functional connectivity changes in takotsubo syndrome. **Figure D** shows functional hypoconnectivity in key pathways involved in autonomic control of cardiac function in takotsubo syndrome.

Supplemental Files

Table 1. Case Description of Takotsubo Syndrome Patients						
Patient	**Symptoms**	**Haemodynamics**	**Cardiac Investigations**	**Trigger**	**Biomarkers**	**Days to MRI**
Patient 1 **56 year old female**	Shortness of breath	BP 103/73 HR 100	ECG: widespread TWI and QTc prolongation Echo: Mid-apical hypokinesis with preservation of basal regions. LVOTO Angio: No obstructive coronary artery disease CMR: No LGE, T2 STIRR in keeping with intense myocardial oedema in apical regions. EF 45%	Physical illness-COPD exacerbation	Trop 3452 ng/L BNP 397 pg/ml CRP 10 mg/L	5 days
Patient 2 **59 year old female**	Syncope	BP 121/72 HR 82	ECG:ST elevation anteriorly Echo: Mid-apical hypokinesis with preservation of basal regions. Angio: No obstructive coronary artery disease CMR: No LGE, T2 STIRR in keeping with intense	No triggers	Trop 1001 ng/L BNP 84 pg/ml CRP 49 mg/L	5 days

			myocardial oedema in apical regions. EF 40%			
Patient 3 **79 year old female**	Chest pain	BP 98/40 HR 64	ECG: widespread TWI and QTc prolongation Echo: Mid-apical hypokinesis with preservation of basal regions. Angio: No obstructive coronary artery disease CMR: No LGE, T2 STIRR in keeping with intense myocardial oedema in apical regions. EF 30%	Emotional stressor	Trop 278 ng/L CRP 3 mg/L	1 days
Patient 4 **69 year old female**	Chest pain	BP 157/86 HR 61	ECG: Ant ST elevation. Echo: Mid-apical hypokinesis with preservation of basal regions. Angio: No obstructive coronary artery disease CMR: No LGE, T2 STIRR in keeping with intense myocardial oedema in	Emotional Stressor	Trop 5663 ng/L BNP 175 pg/ml CRP 7 mg/L	1 days

			apical regions. EF 45%			
Patient 5 **56 year old female**	Chest pain	BP 158/101 HR 80	ECG: widespread TWI and QTc prolongation Echo: Mid-apical hypokinesis with preservation of basal regions. Angio: No obstructive coronary artery disease CMR: No LGE, T2 STIRR in keeping with intense myocardial oedema in apical regions. EF 50%	Emotional Stressor	Trop 44ng/L BNP 6 pg/ml CRP 2 mg/L	1 days
Patient 6 **74 year old female**	Chest pain	BP 120/78 HR 76	ECG: Anterior ST elevation Echo: Mid-chamber hypokinesis with preservation of basal and apical regions. Angio: No obstructive coronary artery disease CMR: No LGE, T2 STIRR in keeping with intense myocardial oedema in mid chamber	Emotional Stressor	Trop 3489 ng/L BNP 71 pg/ml CRP 7 mg/L	1 days

			regions. EF 50%			
Patient 7 **61 year old female**	Shortness of breath	BP 125/64 HR 79	ECG: widespread TWI and QTc prolongation Echo: Mid-apical hypokinesis with preservation of basal regions. Angio: No obstructive coronary artery disease CMR: No LGE, T2 STIRR in keeping with intense myocardial oedema in apical regions. EF 30%	No trigger	Trop 932 ng/L BNP 300 pg/ml CRP 2 mg/L	4 days
Patient 8 **74 year old female**	Chest pain	BP 161/115 HR 90	ECG: widespread TWI and QTc prolongation Echo: Mid-apical hypokinesis with preservation of basal regions. Angio: No obstructive coronary artery disease CMR: No LGE, T2 STIRR in keeping with intense myocardial oedema in	No trigger	Trop 831 ng/L BNP 52 pg/ml CRP 4 mg/L	5 days

			apical regions. EF 43%			
Patient 9 **55 year old man**	Chest pain	BP 138/97 HR 88	ECG: Inferior ST elevation Echo: Mid-apical hypokinesis with preservation of basal regions. Angio: No obstructive coronary artery disease CMR: mid-wall LGE in inferolateral wall at hinge point, T2 STIRR in keeping with intense myocardial oedema in apical regions. EF 50%	Emotional Stressor	Trop 7396 ng/L BNP 36 pg/ml CRP 5 mg/L	4 days
Patient 10 **67 year old female**	Chest pain	BP 100/72 HR 60	ECG: widespread TWI and QTc prolongation Echo: Mid-apical hypokinesis with preservation of basal regions. Angio: No obstructive coronary artery disease CMR: No LGE, T2 STIRR in keeping with intense myocardial	No trigger	Trop 1173 ng/L BNP 62 pg/ml CRP 1 mg/L	5 days

			oedema in apical regions. EF 35%			
Patient 11 **71 year old female**	Chest pain	BP 153/86 HR 93	ECG: widespread TWI and QTc prolongation Echo: Mid-apical hypokinesis with preservation of basal regions. Angio: No obstructive coronary artery disease CMR: No LGE, T2 STIRR in keeping with intense myocardial oedema in apical regions. EF 39%	Physical illness-acute cholecystitis	Trop 443 ng/L BNP 322 pg/ml CRP 9 mg/L	7 days
Patient 12 **69 year old female**	Chest pain	BP 157/92 HR 67	ECG: widespread TWI and QTc prolongation Echo: Mid-apical hypokinesis with preservation of basal regions. Angio: No obstructive coronary artery disease CMR: No LGE, T2 STIRR in keeping with intense myocardial	No trigger	Trop 587ng/L BNP 47 pg/ml CRP 1 mg/L	8 days

			oedema in apical regions. EF 58%			
Patient 13 **83 year old female**	Syncope	BP 85/57 HR 75	ECG:widespread TWI and QTc prolongation Echo: Mid-apical hypokinesis with preservation of basal regions. Angio:No obstructive coronary artery disease CMR: No LGE, T2 STIRR in keeping with intense myocardial oedema in apical regions. EF 47%	No trigger	Trop 1984 ng/L CRP 45 mg/L	8 days
Patient 14 **63 year old female**	Chest pain	BP 60/40 HR 63	ECG: Anterior ST elevation Echo: Mid-apical hypokinesis with preservation of basal regions. LVOTO Angio:No obstructive coronary artery disease CMR: No LGE, T2 STIRR in keeping with intense myocardial oedema in	Emotional Stressor	Trop 2381 ng/L BNP 484pg/ml CRP 8 mg/L	9 days

			apical regions. EF 40%			
Patient 15 **74 year old female**	Chest pain	BP 140/66 HR 62	ECG:widespread TWI and QTc prolongation Echo: Mid-apical hypokinesis with preservation of basal regions. LVOTO Angio:No obstructive coronary artery disease CMR: No LGE, T2 STIRR in keeping with intense myocardial oedema in apical regions. EF 45%	Emotional trigger	Trop 721 ng/L BNP 33 pg/ml CRP 1 mg/L	4 days
Patient 16 **62 year old female**	Chest pain	BP 127/74 HR 56	ECG: Ant ST elevation Echo: Mid-cavity hypokinesis with preservation of basal and apical regions. Angio:No obstructive coronary artery disease CMR: No LGE, T2 STIRR in keeping with intense myocardial oedema in mid	Physical exertion	Trop 2113 ng/L BNP 52 pg/ml CRP 2 mg/L	1 days

			cavity regions. EF 47%			
Patient 17 **73 year old female**	Chest pain	BP 135/90 HR 74	ECG:widespread TWI and QTc prolongation Echo: Mid-apical hypokinesis with preservation of basal regions. Angio:No obstructive coronary artery disease CMR: No LGE, T2 STIRR in keeping with intense myocardial oedema in apical regions. EF 40%	No trigger	Trop 6685 ng/L CRP 1 mg/L	2 days
Patient 18 **72 year old female**	Abdominal pain	BP 131/60 HR 95	ECG:widespread TWI and QTc prolongation Echo: Mid-cavity hypokinesis with preservation of basal and apical regions. Angio:No obstructive coronary artery disease CMR: No LGE, T2 STIRR in keeping with intense myocardial	Physical illness-diarrhea and vomiting	Trop 391ng/L BNP 94 pg/ml CRP 2 mg/L	2 days

			oedema in mid cavity regions. EF 30%			
Patient 19 **75 year old female**	Chest pain	BP 128/84 HR 99	ECG:Ant ST elevation Echo: Mid-apical hypokinesis with preservation of basal regions. Angio:No obstructive coronary artery disease CMR: No LGE, T2 STIRR in keeping with intense myocardial oedema in apical regions. EF 50%	Physical illness-flu like symptoms	Trop 5417 ng/L CRP 10 mg/L	6 days
Patient 20 **60 year old female**	Chest pain	BP 108/72 HR 82	ECG:widespread TWI and QTc prolongation Echo: Mid-apical hypokinesis with preservation of basal regions. Angio:No obstructive coronary artery disease CMR: No LGE, T2 STIRR in keeping with intense myocardial oedema in	Emotional trigger	Trop 106 ng/L BNP 14 pg/ml CRP 2 mg/L	9 days

			apical regions. EF 40%			
Patient 21 **53 year old female**	Chest pain	BP 123/83 HR 75	ECG: widespread TWI and QTc prolongation Echo: Mid cavity hypokinesis with preservation of basal and apical regions. Angio:No obstructive coronary artery disease CMR: No LGE, T2 STIRR in keeping with intense myocardial oedema in mid cavity regions. EF 55%	Physical illness-adverse reaction to COVID vaccine	Trop 1662 ng/L BNP 67 pg/ml CRP 1 mg/L	9 days
Patient 22 **72 year old female**	Chest pain	BP 151/78 HR 72	ECG: Ant ST elevation Echo: Mid-apical hypokinesis with preservation of basal regions. Angio: No obstructive coronary artery disease CMR: No LGE, T2 STIRR in keeping with intense myocardial oedema in	No trigger	Trop 12100 ng/L BNP 205 pg/ml CRP 2 mg/L	5 days

			apical regions. EF 50%			
Patient 23 **68 year old female**	Chest pain	BP 133/71 HR 76	ECG: Ant St elevation Echo: Mid-apical hypokinesis with preservation of basal regions. Angio: No obstructive coronary artery disease CMR: No LGE, T2 STIRR in keeping with intense myocardial oedema in apical regions. EF 45%	Emotional trigger	Trop 1781 ng/L BNP 49 pg/ml CRP 35 mg/L	16 days
Patient 24 **67 year old female**	Syncope	BP 131/81 HR 71	ECG: Ant ST elevation Echo: Mid-apical hypokinesis with preservation of basal regions. LVOTO Angio:No obstructive coronary artery disease CMR: No LGE, T2 STIRR in keeping with intense myocardial oedema in apical regions. EF 40%	No trigger	Trop 1750 ng/L CRP 2 mg/L	3 days

Patient 25 **47 year old female**	Chest pain	BP 125/72 HR 84	ECG: widespread TWI and QTc prolongation Echo: focal anterior wall hypokinesis Angio: No obstructive coronary artery disease CMR: No LGE, T2 STIRR in keeping with myocardial oedema in anterior regions. EF 55%	No trigger	Trop 38ng/L CRP 5 mg/L	10 days

Table 2. White matter hyperintensities

	Acute Takotsubo	Matched Controls	P Value
Total volume (ml)	6.52±10.25	5.91±13.40	0.857
Number of Lesions	11.52±6.28	14.92±17.01	0.353

Data is shown as mean±SD

Table 3. Brain surface areas

Surface Area of individual brain regions (mm2)	Acute Takotsubo	Matched Controls	P value	P value (corrected)
Right Caudal Anterior Cingulate	658±119	652±108	0.338	NS
Left Caudal Anterior Cingulate	573±119	579±141	0.239	NS
Right Caudal Middle Frontal	1844±278	1893±266	<0.001	<0.001
Left Caudal Middle Frontal	1975±320	1948±322	<0.001	0.001
Right Cuneus	1461±180	1511±227	0.009	0.61
Left Cuneus	1372±170	1468±261	0.053	NS
Right Entorhinal	359±78	358±70	0.002	0.13
Left Entorhinal	397±72	399±75	0.008	0.54
Right Fusiform	2629±301	2667 ±322	<0.001	<0.001
Left Fusiform	2741±251	2767±293	<0.001	<0.001
Right Inferiorparietal	4461±619	4488±498	0.005	0.34
Left Inferiorparietal	3961±638	3746±456	<0.001	0.03
Right Inferiortemporal	2847±364	2834±328	0.002	0.13
Left Inferiortemporal	3029±420	2893±344	<0.001	0.03
Right Isthmus Cingulate	865±89	829±99	0.012	0.81
Left Isthmus Cingulate	924±146	932±131	0.045	NS
Right Lateral Occiptal	4492±610	4561±513	0.043	NS
Left Lateral Occipital	4438±516	4623±601	0.008	0.54
Right Lateral Orbitofrontal	2393±299	2377±243	0.002	0.13
Left Lateral Orbitofrontal	2396±235	2376±315	<0.001	0.01
Right Lingual	2911±316	2970±306	0.071	NS
Left Lingual	2722±352	2872±347	0.090	NS
Right Medial Orbitofrontal	1883±196	1920±202	<0.001	0.04
Left Medial Orbitofrontal	17523±187	1798±190	0.002	0.13
Right Middle Temporal	3054±335	3039±229	<0.001	<0.001
Left Middle Temporal	2785±323	2710±242	0.004	0.272
Right Parrahippocampal	556±56	562±53	0.001	0.07

Left Parrahippocampal	587±76	581±64	0.374	NS
Right Paracentral	1354±147	1414±154	0.002	0.13
Left Paracentral	1177±115	1236±123	<0.001	<0.001
Right Parsopercularis	1229±165	1227±176	<0.001	0.053
Left Parsopercularis	1424±128	1456±219	0.309	NS
Right Parsorbitalis	749±95	766±78	0.018	NS
Left Parsorbitalis	607±90	631±90	<0.001	0.002
Right Parstriangularis	1370±175	1329±157	0.017	NS
Left Parstriangularis	1147±159	1175±166	0.175	NS
Right Pericalcarine	1460±269	1467±288	0.170	NS
Left Pericalcarine	1271±247	1326±272	0.335	NS
Right Postcentral	3564±275	3547±269	0.001	0.07
Left Postcentral	3661±330	3686±366	<0.001	0.063
Right Posterior Cingulate	1014±124	1060±126	0.162	NS
Left Posterior Cingulate	994±161	1051±115	0.015	NS
Right Precentral	4227±449	4360±477	<0.001	<0.001
Left Precentral	4221±497	4333±391	<0.001	<0.001
Right Precuneus	3527±351	3519±419	<0.001	0.003
Left Precuneus	3422±321	3465±379	<0.001	0.001
Right Rostral Anterior Cingulate	500±93	540±85	0.043	NS
Left Rostral Anterior Cingulate	738±159	755±171	<0.001	0.007
Right Rostral Middle Frontal	4888±516	5061±571	<0.001	0.007
Left Rostral Middle Frontal	4688±571	4777±657	<0.001	<0.001
Right Superior Frontal	6109±620	6222±653	<0.001	<0.001
Left Superior Frontal	6286±648	6367±519	<0.001	<0.001
Right Superior Parietal	4756±411	4905±581	<0.001	<0.001
Left Superior Parietal	4951±438	4901±674	0.003	0.204
Right Superior Temporal	3241±263	3362±332	0.001	0.068
Left Superior Temporal	3455±271	3519±325	0.002	0.136
Right Supramarginal	3146±319	3276±494	<0.001	0.037
Left Supramarginal	3463±459	3666±434	<0.001	0.033
Right Frontal Pole	321±36	326±30	0.008	0.544

Left Frontal Pole	267±38	262±30	0.007	0.476
Right Temporal Pole	473±51	457±57	0.505	NS
Left Temporal Pole	470±46	471±57	0.005	0.343
Right Transverse Temporal	289±29	305±48	0.004	0.272
Left Transverse Temporal	406±44	411±68	0.280	NS
Right Insula	2064±239	2132±269	<0.001	<0.001
Left Insula	2206±262	2278±310	<0.001	<0.001
Total Right White Surface Area	75441±5173	76689±5795	<0.001	<0.001
Total Left White Surface Area	75379±5099	76321±5721	<0.001	<0.001

Data is shown as mean±SD and p values are obtained after correction for total brain volume, age, gender. Corrected p value is post Bonferroni correction.

Table 4. Brain Cortical Thickness

Cortical Thickness of individual brain regions	Acute Takotsubo	Matched Controls	P value	P value (corrected)
Right Caudal Anterior Cingulate	2.38±0.21	2.27±0.18	0.016	NS
Left Caudal Anterior Cingulate	2.45±0.22	2.41±0.23	0.814	NS
Right Caudal Middle Frontal	2.44±0.17	2.43±0.11	<0.001	<0.001
Left Caudal Middle Frontal	2.46±0.14	2.44±0.18	<0.001	0.011
Right Cuneus	1.80±0.12	1.78±0.13	0.007	0.476
Left Cuneus	1.77±0.15	1.75±0.12	0.022	NS
Right Entorhinal	3.29±0.29	3.17±0.27	0.631	NS
Left Entorhinal	3.15±0.29	3.07±0.22	0.746	NS
Right Fusiform	2.66±0.16	2.59±0.13	<0.001	<0.001
Left Fusiform	2.64±0.13	2.58±0.14	<0.001	<0.001
Right Inferiorparietal	2.37±0.12	2.32±0.11	<0.001	<0.001
Left Inferiorparietal	2.39±0.11	2.33±0.13	<0.001	<0.001
Right Inferiortemporal	2.70±0.14	2.57±0.15	<0.001	0.002
Left Inferiortemporal	2.67±0.13	2.62±0.13	<0.001	0.020
Right Isthmus Cingulate	2.25±0.15	2.28±0.14	0.926	NS
Left Isthmus Cingulate	2.27±0.16	2.27±0.14	0.547	NS
Right Lateral Occiptal	2.13±0.15	2.11±0.12	<0.001	<0.001
Left Lateral Occipital	2.08±0.17	2.10±0.10	<0.001	<0.001
Right Lateral Orbitofrontal	2.51±0.16	2.52±0.11	<0.001	<0.001
Left Lateral Orbitofrontal	2.52±0.15	2.56±0.14	<0.001	0.001
Right Lingual	1.91±0.12	1.90±0.12	<0.001	0.061
Left Lingual	1.88±0.14	1.87±0.12	<0.001	<0.001
Right Medial Orbitofrontal	2.43±0.22	2.34±0.13	<0.001	0.025
Left Medial Orbitofrontal	2.27±0.15	2.23±0.12	0.032	NS
Right Middle Temporal	2.73±0.15	2.67±0.11	<0.001	<0.001
Left Middle Temporal	2.69±0.16	2.65±0.12	<0.001	0.001
Right Parrahippocampal	2.59±0.21	2.69±0.23	0.015	NS

Left Parrahippocampal	2.70±0.32	2.77±0.30	0.140	NS
Right Paracentral	2.33±0.14	2.26±0.16	<0.001	0.040
Left Paracentral	2.35±0.14	2.30±0.17	<0.001	<0.001
Right Parsopercularis	2.45±0.11	2.50±0.11	<0.001	<0.001
Left Parsopercularis	2.45±0.15	2.45±0.12	<0.001	<0.001
Right Parsorbitalis	2.56±0.15	2.62±0.13	0.002	0.136
Left Parsorbitalis	2.60±0.22	2.54±0.23	0.019	NS
Right Parstriangularis	2.33±0.16	2.37±0.10	<0.001	0.001
Left Parstriangularis	2.33±0.14	2.33±0.12	0.007	0.476
Right Pericalcarine	1.54±0.14	1.52±0.15	0.008	0.544
Left Pericalcarine	1.49±0.12	1.45±0.11	0.020	NS
Right Postcentral	1.98±0.12	1.94±0.12	<0.001	<0.001
Left Postcentral	1.99±0.13	1.97±0.10	<0.001	<0.001
Right Posterior Cingulate	2.41±0.13	2.36±0.13	0.005	0.34
Left Posterior Cingulate	2.38±0.10	2.33±0.14	0.032	NS
Right Precentral	2.44±0.12	2.44±0.16	<0.001	<0.001
Left Precentral	2.47±0.11	2.46±0.13	<0.001	<0.001
Right Precuneus	2.31±0.13	2.25±0.11	<0.001	<0.001
Left Precuneus	2.31±0.11	2.25±0.13	<0.001	<0.001
Right Rostral Anterior Cingulate	2.78±0.22	2.63±0.18	0.030	NS
Left Rostral Anterior Cingulate	2.63±0.23	2.59±0.18	0.043	NS
Right Rostral Middle Frontal	2.25±0.12	2.28±0.10	<0.001	<0.001
Left Rostral Middle Frontal	2.26±0.10	2.24±0.09	<0.001	<0.001
Right Superior Frontal	2.61±0.13	2.58±0.10	<0.001	<0.001
Left Superior Frontal	2.57±0.13	2.58±0.10	<0.001	<0.001
Right Superior Parietal	2.10±0.12	2.07±0.12	<0.001	<0.001
Left Superior Parietal	2.13±0.13	2.10±0.12	<0.001	<0.001
Right Superior Temporal	2.65±0.19	2.64±0.10	<0.001	<0.001
Left Superior Temporal	2.65±0.17	2.61±0.13	<0.001	<0.001
Right Supramarginal	2.44±0.13	2.41±0.10	<0.001	<0.001
Left Supramarginal	2.49±0.11	2.45±0.11	<0.001	<0.001
Right Frontal Pole	2.60±0.21	2.63±0.25	0.179	NS

Left Frontal Pole	2.61±0.27	2.63±0.19	0.004	0.272
Right Temporal Pole	3.61±0.27	3.61±0.28	0.130	NS
Left Temporal Pole	3.66±0.23	3.51±0.37	<0.001	0.052
Right Transverse Temporal	2.26±0.20	2.26±0.21	0.003	0.204
Left Transverse Temporal	2.25±0.20	2.25±0.18	<0.001	0.004
Right Insula	2.89±0.19	2.79±0.11	<0.001	<0.001
Left Insula	2.87±0.16	2.77±0.23	0.007	0.476
Total Right Mean Thickness	2.37±0.10	2.35±0.09	<0.001	<0.001
Total Left Mean Thickness	2.38±0.10	2.35±0.08	<0.001	<0.001

Data is shown as mean±SD and p values are obtained after correction for total brain volume, age, gender. Corrected p value is post Bonferroni correction.

Table 5. Total, haemispheric and regional limbic centres' brain volumes.

Brain volume (hemispheric/regional) (mm3)	Acute Takotsubo	Matched Controls	P value	P value (corrected)
Left Hemisphere Cerebral White Matter	206389±20883	212789±21526	<0.001	<0.001
Right Hemisphere Cerebral White Matter	204953±20251	212146±20692	<0.001	<0.001
Total Cerebral White Matter	411342±41051	424934±41984	<0.001	<0.001
Total Gray Matter	540388±41158	539419±35543	<0.001	<0.001
Subcortical Gray Matter	49679±4087	50154±2784	<0.001	<0.001
Left Thalamus	6235±680	6135±437	<0.001	<0.001
Right Thalamus	6020±660	5958±430	<0.001	<0.001
Total Thalamus	12256±1297	12092±827	<0.001	<0.001
Left Hippocampus	3656±358	3768±273	<0.001	<0.001
Right Hippocampus	3731±361	3840±308	<0.001	<0.001
Total Hippocampus	7387±702	7608±556	<0.001	<0.001
Left Amygdala	1374±233	1417±153	0.002	0.078
Right Amygdala	1560±170	1562±190	0.007	0.273
Total Amygdala	2935±384	2979±318	0.002	0.078
Left Caudate	2994±341	3055±343	0.004	0.156
Right Caudate	3110±403	3236±360	<0.001	0.037
Total Caudate	6104±723	6291±683	0.001	0.039
Left Accumbens	393±106	457±79	0.008	0.312
Right Accumbens	476±92	497±79	0.027	NS
Total Accumbens	869±188	955±140	0.008	0.312
Left Caudal Anterior Cingulate	1511±402	1493±390	0.260	NS
Right Caudal Anterior Cingulate	1774±350	1694±263	0.100	NS
Total Caudal Anterior Cingulate	3285±552	3187±576	0.953	NS
Left Isthmus Cingulate Volume	2244±377	2286±295	0.012	0.468
Right Isthmus Cingulate Volume	2157±216	2117±253	0.01	0.39
Total Isthmus Cingulate Volume	4401±515	4402±474	0.003	0.117

Left Posterior Cingulate Volume	2544±405	2620±283	0.004	0.156
Right Posterior Cingulate Volume	2629±353	2705±276	0.348	NS
Total Posterior Cingulate Volume	5173±633	5325±499	<0.001	<0.001
Left Rostral Anterior Cingulate	2228±509	2196±504	0.017	0.663
Right Rostral Anterior Cingulate	1607±3156	1655±282	0.238	NS
Total Rostral Anterior Cingulate	3835±713	3851±701	0.027	NS
Left Parahippocampus	1828±263	1895±280	0.006	0.234
Right Parahippocampus	1676±244	1778±202	<0.001	<0.001
Total Parahippocampus	3504±472	3674±458	<0.001	0.007
Left Insula	6342±841	6139±773	<0.001	<0.001
Right Insula	6047±754	5902±703	<0.001	<0.001
Total Insula	12389±1574	12042±1415	<0.001	<0.001
Brainstem	18782±1966	19394±1956	<0.001	<0.001

Data is shown as mean±SD and p values are obtained after correction for total brain volume, age, gender and photoperiod. Corrected p value is post Bonferroni correction.

Table 1. Baseline Characteristic in Patients with Takotsubo Syndrome and Matched Controls			
	Takotsubo Patients n=25	Matched Controls n=25	P-value
Age	68 (47-83)	65 (64-69)	0.809
Gender			1.0
Female	24(96%)	24(96%)	
Past medical history			
Hypertension	8(32%)	6 (24%)	0.538
Diabetes	2(8%)	3 (12%)	0.646
Stroke	1(4%)	1 (4%)	1.0
Thyroid disease	2(8%)	2 (8%)	1.0
Psychiatric disease	6(24%)	4 (16%)	0.490
Atrial fibrillation	2(8%)	0 (0%)	0.155
Chronic Obstructive Pulmonary Disease	5(20%)	0 (0%)	0.018
Takotsubo trigger type			
Emotional	10(40%)		
Physical	7(28%)		
None	8(32%)		
Days from symptom onset to MRI	5(2-8)		
Left ventricular ejection fraction on admission (%)	45±8.34		
Medications			
Beta-Blocker	17(68%)	2 (8%)	<0.001
ACE-Inhibitor	16(64%)	1 (4%)	<0.001
Angiotensin Receptor Blocker	2(8%)	2 (8%)	1.0
Mineralocorticoid Antagonist	4(16%)	0 (0%)	0.038
Calcium Channel Blocker	3(12%)	2 (8%)	0.646
Anti-Platelets	15(60%)	2 (8%)	<0.001
Anticoagulants	4(16%)	0 (0%)	0.038
Diuretic	4(16%)	3 (12%)	0.691
Statin	17(68%)	2 (8%)	<0.001
Hypoglycaemic Drugs	3(12%)	1 (4%)	0.561
Nitrates	3(12%)	1 (4%)	0.307
Antidepressants	4(16%)	2 (8%)	0.394
Antipsychotics	0(0%)	0 (0%)	1.0
Validated questionnaires scores			
HADS	13.20±10.30	3.68±2.43	<0.001
Eysenck Extraversion	10.72±5.09	13.34±7.18	0.143
Eysenck Introversion	12.28±5.09	9.66±7.18	0.143
Eysenck Neuroticism	9.52±5.5	7.28±6.45	0.191
Eysenck Stability	14.48±5.5	16.72±6.45	0.191

Data is shown as frequencies n (%), or mean (IQR) or mean±SD.

Table 2. Brain parameters				
White matter hyperintensities (mm)	Acute Takotsubo	Matched Controls	P value	P value (corrected)
Total volume (ml)	6.52±10.25	5.91±13.40	0.857	0.857
Number of Lesions	11.52±6.28	14.92±17.01	0.353	0.353
Surface Area of individual brain regions (mm2)				
Right Isthmus Cingulate	865±89	829±99	0.012	0.81
Left Isthmus Cingulate	924±146	932±131	0.045	NS
Right Parrahippocampal	556±56	562±53	0.001	0.07
Left Parrahippocampal	587±76	581±64	0.374	NS
Right Rostral Anterior Cingulate	500±93	540±85	0.043	NS
Left Rostral Anterior Cingulate	738±159	755±171	<0.001	0.007
Right Insula	2064±239	2132±269	<0.001	<0.001
Left Insula	2206±262	2278±310	<0.001	<0.001
Total Right White Surface Area	75441±5173	76689±5795	<0.001	<0.001
Total Left White Surface Area	75379±5099	76321±5721	<0.001	<0.001
Cortical Thickness of individual brain regions (cm)				
Right Caudal Anterior Cingulate	2.38±0.21	2.27±0.18	0.016	NS
Left Caudal Anterior Cingulate	2.45±0.22	2.41±0.23	0.814	NS
Right Rostral Anterior Cingulate	2.78±0.22	2.63±0.18	0.030	NS
Left Rostral Anterior Cingulate	2.63±0.23	2.59±0.18	0.043	NS
Right Insula	2.89±0.19	2.79±0.11	<0.001	<0.001
Left Insula	2.87±0.16	2.77±0.23	0.007	0.476
Total Right Mean Thickness	2.37±0.10	2.35±0.09	<0.001	<0.001
Total Left Mean Thickness	2.38±0.10	2.35±0.08	<0.001	<0.001
Brain volume (hemispheric/regional) (mm3)				
Total Cerebral White Matter	411342±41051	424934±41984	<0.001	<0.001
Total Gray Matter	540388±41158	539419±35543	<0.001	<0.001
Subcortical Gray Matter	49679±4087	50154±2784	<0.001	<0.001
Left Thalamus	6235±680	6135±437	<0.001	<0.001
Right Thalamus	6020±660	5958±430	<0.001	<0.001
Total Thalamus	12256±1297	12092±827	<0.001	<0.001
Left Hippocampus	3656±358	3768±273	<0.001	<0.001
Right Hippocampus	3731±361	3840±308	<0.001	<0.001
Total Hippocampus	7387±702	7608±556	<0.001	<0.001
Left Amygdala	1374±233	1417±153	0.002	0.078
Right Amygdala	1560±170	1562±190	0.007	0.273
Total Amygdala	2935±384	2979±318	0.002	0.078
Left Caudate	2994±341	3055±343	0.004	0.156
Right Caudate	3110±403	3236±360	<0.001	0.037
Total Caudate	6104±723	6291±683	0.001	0.039
Left Accumbens	393±106	457±79	0.008	0.312
Right Accumbens	476±92	497±79	0.027	NS
Total Accumbens	869±188	955±140	0.008	0.312
Left Isthmus Cingulate Volume	2244±377	2286±295	0.012	0.468
Right Isthmus Cingulate Volume	2157±216	2117±253	0.01	0.39
Total Isthmus Cingulate Volume	4401±515	4402±474	0.003	0.117
Left Parahippocampus	1828±263	1895±280	0.006	0.234
Right Parahippocampus	1676±244	1778±202	<0.001	<0.001
Total Parahippocampus	3504±472	3674±458	<0.001	0.007
Left Insula	6342±841	6139±773	<0.001	<0.001
Right Insula	6047±754	5902±703	<0.001	<0.001
Total Insula	12389±1574	12042±1415	<0.001	<0.001
Brainstem	18782±1966	19394±1956	<0.001	<0.001

Data is shown as mean±SD and p values are obtained after correction for total brain volume, age, gender and photoperiod**.** Corrected P values are post Bonferroni correction.

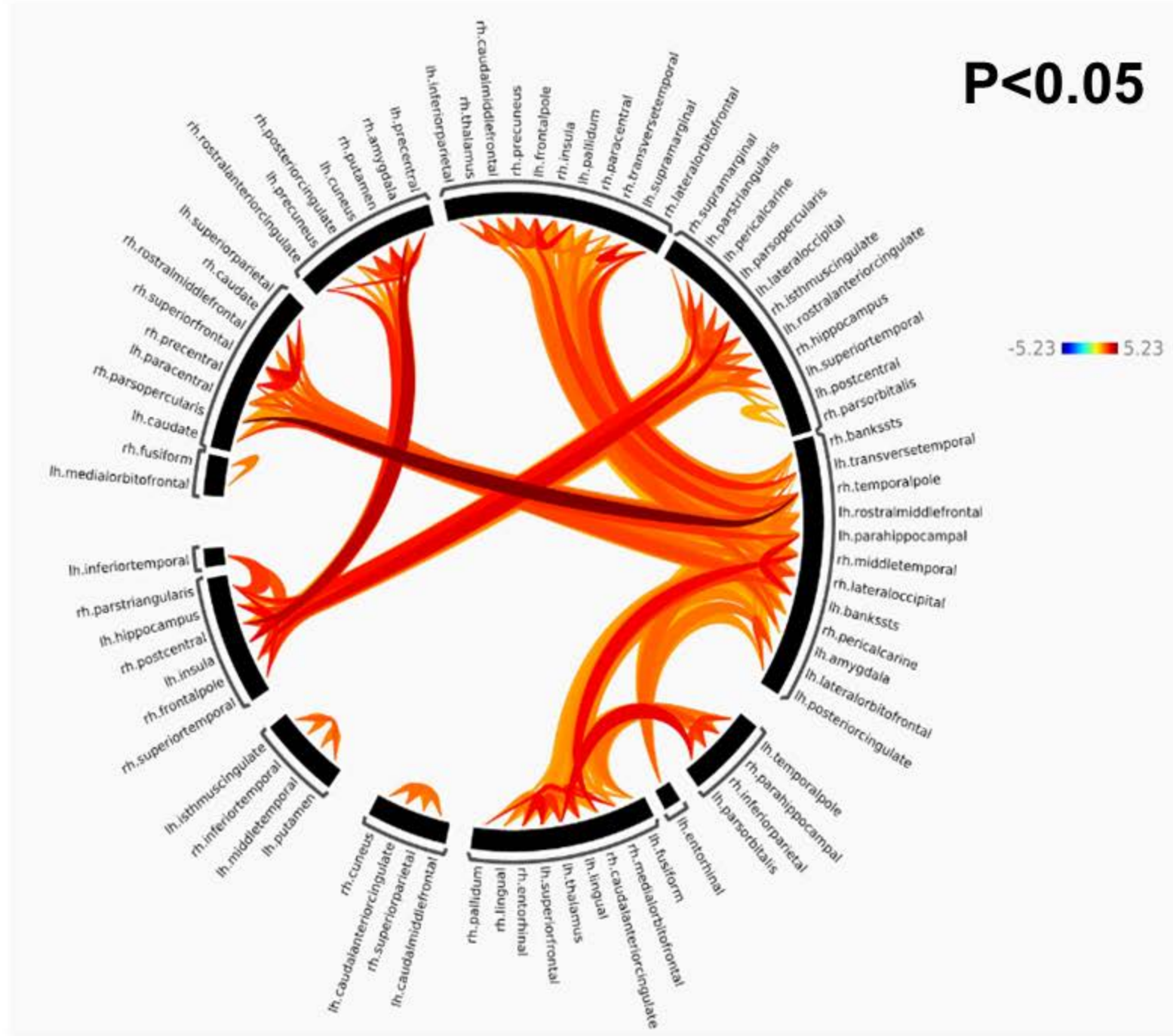
P<0.05
-5.23
5.23
lh.caudalmiddlefrontal
rh.thalamus
lh.inferiorparietal
rh.precuneus
lh.frontalpole
rh.insula
lh.pallidum
rh.paracentral
lh.transversetemporal
rh.supramarginal
lh.lateralorbitofrontal
lh.supramarginal
rh.parstriangularis
lh.pericalcarine
lh.parsopercularis
rh.lateraloccipital
rh.isthmuscingulate
lh.rostralanteriorcingulate
rh.hippocampus
lh.superiortemporal
lh.postcentral
rh.parsorbitalis
rh.bankssts
lh.transversetemporal
rh.temporalpole
lh.rostralmiddlefrontal
lh.parahippocampal
rh.middletemporal
rh.lateraloccipital
lh.bankssts
rh.pericalcarine
lh.amygdala
lh.lateralorbitofrontal
lh.posteriorcingulate
lh.temporalpole
rh.parahippocampal
rh.inferiorparietal
lh.parsorbitalis
lh.entorhinal
lh.fusiform
rh.medialorbitofrontal
rh.caudalanteriorcingulate
lh.lingual
lh.thalamus
lh.superiorfrontal
rh.entorhinal
rh.lingual
rh.pallidum
rh.caudalmiddlefrontal
lh.superiorparietal
lh.caudalanteriorcingulate
rh.cuneus
lh.isthmuscingulate
rh.inferiortemporal
lh.middletemporal
lh.putamen
rh.superiortemporal
rh.frontalpole
lh.insula
rh.postcentral
rh.hippocampus
rh.parstriangularis
lh.inferiortemporal
lh.medialorbitofrontal
rh.fusiform
lh.caudate
rh.parsopercularis
lh.paracentral
rh.precentral
rh.superiorfrontal
rh.rostralmiddlefrontal
rh.caudate
lh.superiorparietal
rh.rostralanteriorcingulate
lh.precuneus
rh.posteriorcingulate
lh.cuneus
rh.putamen
rh.amygdala
lh.precentral

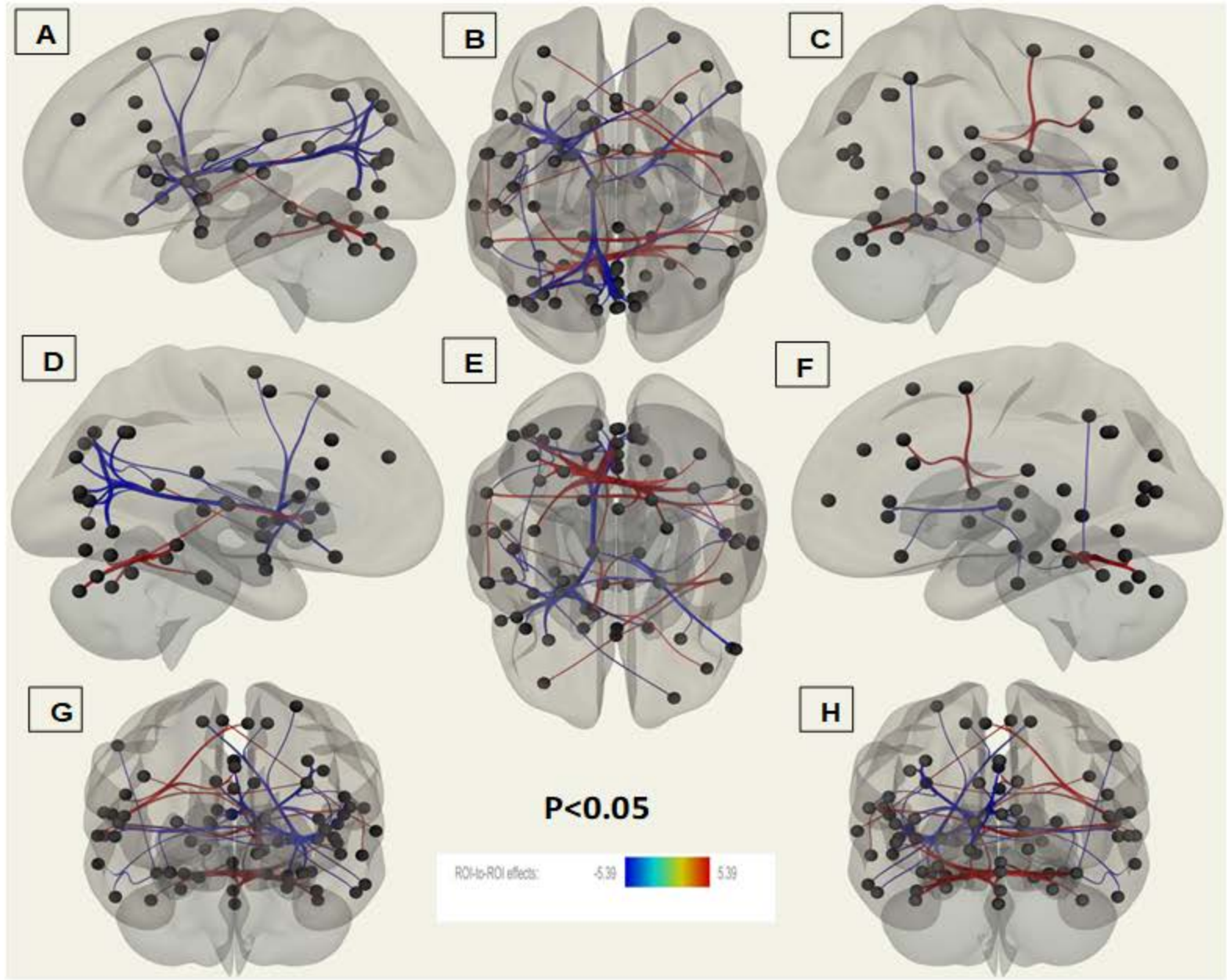
A
B
C
D
E
F
G
H
P<0.05
ROI-to-ROI effects:
-5.39
5.39

A

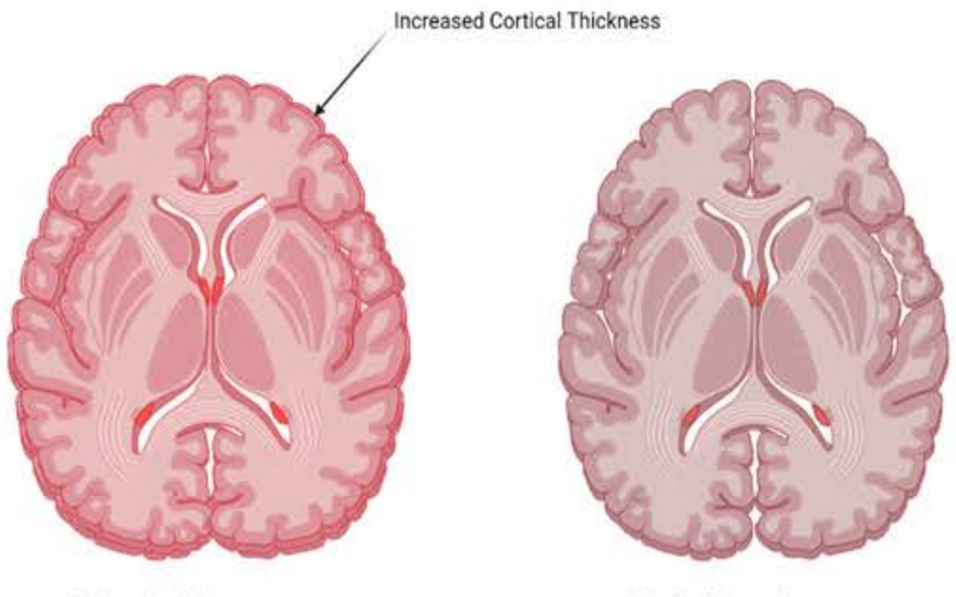

B

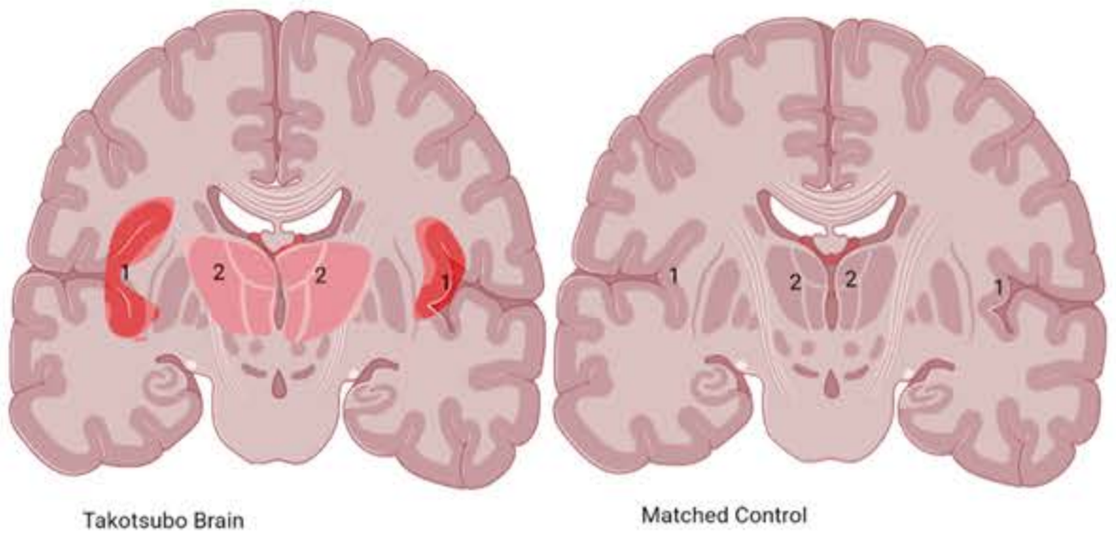

1=Insula
2=Thalamus

C

Structural Connectivity

Functional Connectivity

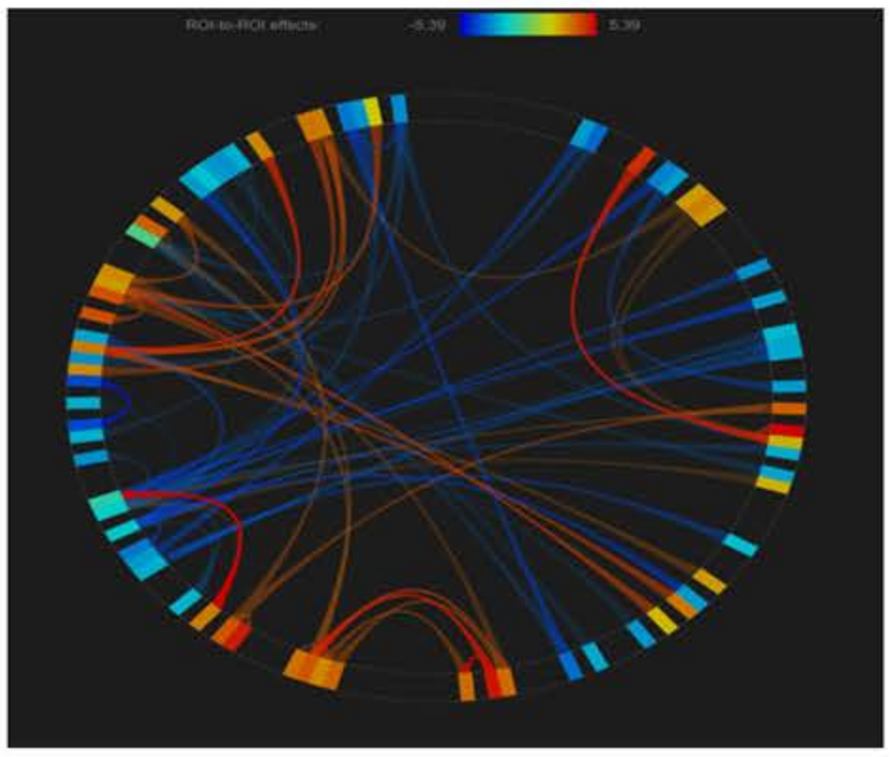

D

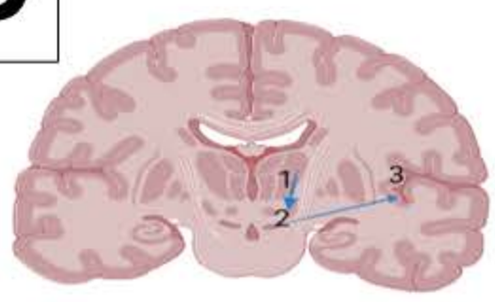

1. Thalamus
2. Amygdala
3. Insula

Abnormal autonomic regulation in acute takotsubo syndrome

Apical ballooning in acute takotsubo syndrome